Comenius University in Bratislava

Faculty of Mathematics, Physics and Informatics

Department of Astronomy, Physics of the Earth, and Meteorology

Diagnostics of the Non-Maxwellian Electron Distributions in the Solar Corona and Transition Region

Dissertation Thesis Report

4.1.7 Astronomy & 4.1.8. Astrophysics

RNDr. Šimon Mackovjak

Bratislava, 2014

Abstract

The non-Maxwellian κ-distributions have been detected in various space plasmas, including solar wind. However, no evidence of their presence in the solar corona has been found yet. The PhD thesis is focused on diagnostics of κ-distributions of electrons in the solar corona and transition region using spectroscopic data. The diagnostic methods were proposed by Dzifčáková and Kulinová (2010) for spectral lines of iron ions. These methods are in PhD thesis extended using lines of other ions. Lines suitable for diagnostics of κ, as well as density and temperature were selected. A specialized observation for the Hinode/EIS instrument were prepared and carried out. This dataset is analyzed and diagnosed parameters of coronal plasma are presented and discussed. The diagnosed results shown that the investigated plasma is unlikely to be Maxwellian. The differential emission measure (DEM) of different solar regions were investigated and the influence of κ-distribution to the DEM were shown. For lower κ, the peaks of the DEMs are typically shifted to higher temperatures and the DEMs themselves become more wider. The PhD thesis provides straightforward analysis from theoretical diagnostic method to application on obtained data. The presented results challenge the traditional Maxwellian analysis of coronal observations. The PhD Thesis Report offers a short introduction to the κ-distributions and the summary of the most important results of the the PhD thesis.

Keywords: solar corona – κ-distributions – spectroscopy – plasma diagnostics – differential emission measure

Contents

Chapter 1

κ-distributions and EUV spectroscopy

1.1 κ-distributions

The main role of the space science is to explore the universe. The observations are in this process absolutely essential. In this sense, the solar physics is a very privileged part of space science, due to its numerous ground and space-borne observatories with a multitude of high-precision data. Despite that, there are many processes which are unresolved and their nature is still too complicated.

The assumption that the energies of the particles in the solar atmosphere are distributed by Maxwellian distribution is commonly used in the scientific community. Most of the present-day observations are interpreted under this assumption, although the non-Maxwellian distributions would offer physically more consistent interpretation. Departures from the Maxwellian distribution are argued to be ubiquitous in the solar atmosphere above $R = 1.05\,R_{\rm Sun}$ (Scudder and Karimabadi, 2013). In this respect, dynamic or nonlocal effects give rise to the κ-distributions characterized by suprathermal, high-energy tails (e.g., Vasyliunas, 1968; Owocki and Scudder, 1983; Shoub, 1983; Leubner, 2002; Tsallis, 2009; Livadiotis and McComas, 2013). The κ-distributions were detected in solar wind (e.g. Collier et al., 1996; Maksimovic et al., 1997; Zouganelis, 2008; Le Chat et al., 2011), outer heliosphere (Decker et al., 2005), inner heliosheath (Livadiotis and McComas, 2012), and also in the solar transition region (e.g., Pinfield et al., 1999; Dzifčáková and Kulinová, 2011) and flare plasmas (Kašparová and Karlický, 2009; Oka et al., 2013). However, direct evidence for the presence of κ-distributions in the solar corona is

still lacking (Feldman et al., 2007) or ambiguous.

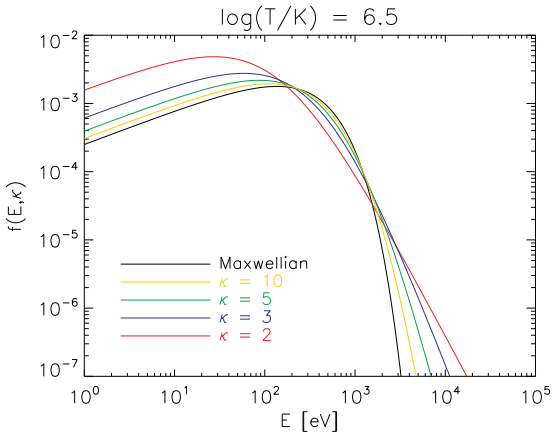

Figure 1.1: A comparison of the κ-distribution with $\kappa = 2$, 3, 5, 10 and the Maxwellian one. The energy distributions are displayed for the same $T = 10^{6.5}$ K and the mean energy.

The κ-distribution (Fig. 1.1) is a distribution of electron energies characterized by a power-law high-energy tail (Owocki and Scudder, 1983; Livadiotis and McComas, 2009)

$$f(E,\kappa)\mathrm{d}E = A_\kappa \frac{2}{\sqrt{\pi}(k_\mathrm{B}T)^{3/2}} \frac{E^{1/2}\mathrm{d}E}{\left(1+\frac{E}{(\kappa-3/2)k_\mathrm{B}T}\right)^{\kappa+1}}\,, \tag{1.1}$$

where A_κ is a normalization constant, k_B is the Boltzmann constant, and T and κ are the parameters of the distribution. The free parameter κ changes the shape of distribution function from $\kappa \to 3/2$ corresponding to the highest deviation from Maxwellian distribution, to $\kappa \to \infty$ corresponding to the Maxwellian distribution.

1.2 EUV synthetic spectra for κ-distributions

We assume that the solar corona is optically thin (e.g., Phillips et al., 2008). The intensity I_{ji} of a spectral line with a wavelength λ_{ji} arising due to a transition $j \to i$ is given by the sum of all contributions from the plasma along the line of sight $\mathrm{d}l$

$$I_{ji} = \frac{1}{4\pi} \int G_{ji}(T, N_\mathrm{e}, \kappa) N_\mathrm{e}^2 \,\mathrm{d}l\,, \tag{1.2}$$

where the contribution function $G_{ji}(T, N_\mathrm{e}, \kappa)$ includes all atomic processes that contribute to the line formation. In optically thin conditions it can be expressed as

$$G_{ji}(T, N_\mathrm{e}, \kappa) = \frac{hc}{\lambda_{ji}} \frac{A_{ji}}{N_\mathrm{e}} \frac{N_{X,i}^{+k}}{N_X^{+k}} \frac{N_X^{+k}}{N_X} A_X \frac{N_\mathrm{H}}{N_\mathrm{e}} \ . \tag{1.3}$$

In this expression, A_{ji} is the Einstein coefficient giving the probability of the spontaneous emission, h is the Planck constant, c is the speed of light, N_e and N_H are the electron and hydrogen densities, respectively, $N_{X,i}^{+k}$ is the density of the k-times ionized ion of the element X with the electron on the excited upper level i, N_X^{+k} is the total density of the ion $+k$, and N_X is the total density of the element X. The quantity $N_{X,i}^{+k}/N_X^{+k}$ represents the excited fraction of the ion $+k$. The N_X^{+k}/N_X is the relative ion abundance and finally $A_X = N_X/N_\mathrm{H}$ is the abundance of the element X.

For evaluating the $G_{ji}(T, N_\mathrm{e}, \kappa)$, the ionization equilibrium (i.e., the N_X^{+k}/N_X) and the excitation equilibrium (i.e., the $N_{X,i}^{+k}/N_X^{+k}$) must be known. Usually, these are obtained by integrating the appropriate cross-sections for collisional ionization, recombination, excitation, and de-excitation over the Maxwellian distribution, as done e.g. in the CHIANTI database (Dere et al., 1997; Landi et al., 2013). However, the $G_{ji}(T, N_\mathrm{e}, \kappa)$ can also be evaluated for the κ-distributions. Generally, the changes in $G_{ji}(T, N_\mathrm{e}, \kappa)$ with κ are dominated by the ionization equilibrium, which exhibits wider and flatter ionization peaks, that can also be shifted to higher or lower temperatures (Dzifčáková, 2002; Dzifčáková and Dudík, 2013). Changes in the electron collisional excitation and deexcitation rates, and therefore in the excitation equilibrium, depend on the type of transitions and ratio of excitation energies to temperature. They can be calculated directly from atomic cross sections; or, if the cross-sections are lacking, using method described in Dzifčáková (2006) and tested in Dzifčáková and Mason (2008).

Using the definition of the differential emission measure (DEM) (e.g., Phillips et al., 2008)

$$DEM(T) = N_\mathrm{e}^2 \frac{\mathrm{d}l}{\mathrm{d}T} \qquad [\mathrm{cm}^{-5}\mathrm{K}^{-1}], \tag{1.4}$$

the observed line intensity can be rewritten as

$$I_{ji} = \frac{1}{4\pi} \int_T G_{ji}(T, N_\mathrm{e}, \kappa) DEM(T)\, \mathrm{d}T. \tag{1.5}$$

The value of $DEM(T)$ can be determined from observed spectra by inversion of Eq. (1.5) using known set of $G_{ji}(T, N_\mathrm{e}, \kappa)$ functions.

Chapter 2

Diagnostics of κ-distributions

2.1 Diagnostics possibilities

We have studied the effects of the non-Maxwellian κ-distributions on the intensities of the spectral lines originating in the solar transition region and the solar corona. This could offers the "missing piece of the puzzle" in the investigation of origin and presence of the κ-distributions in our solar system plasma. Successful diagnostics of κ-distributions could be also important for interpretation of the conditions in the solar corona.

Dzifčáková and Kulinová (2010) proposed a method for the diagnostics of the κ-distributions in the solar corona using spectral lines of iron ions. We extended this analysis and we analyzed the possibilities to diagnose the non-Maxwellian κ-distributions using the Al, Ar, Ca, Mg, Ni, O, S, and Si lines observed by the Extreme-Ultraviolet Imaging Spectrometer (EIS) (Culhane et al., 2007) onboard of the Hinode satellite (Kosugi et al., 2007). From these lines, only Ca, Ni, S, and O lines provide opportunities to determine the value of κ. We discussed the dependence of these κ-sensitive line ratios on the electron density and assessed the presence of possible blends and their elimination. Generally, the line ratios belonging to ions in different ionization stages offer greater diagnostic capabilities. The line ratios of O IV ion are a notable exception. This is the only ion whose lines are density-insensitive and thus also offers diagnostics of κ independent of the electron density. However, simultaneous diagnostics of both temperature and κ is not unique for the entire temperature range. To test the proposed diagnostic methods, the predicted line ratios were compared with the observed line ratios by Brown et al. (2008) in different solar regions. The observed line ratio O IV (207.18 + 207.24 Å) / O IV 279.93 Å does not correspond to the Maxwellian distribution. However, these lines are blended by Mg IX lines.

These blends cannot be removed using EIS observations alone. The observed S X ratios for the limb region suggests $\kappa \leq 3$. However, the limb region is also likely to be multithermal and the error due to photon statistics is large. The data of Brown et al. (2008) are not really appropriate for determination of the value of κ.

We also investigated the influence of κ on the density diagnostics using the line ratios of S X, S XI, Si X, Ar XIV, and Ni XVI proposed by Young (2007). We have found that S X 196.81 Å / 264.23 Å and Si X 261.06 Å / 258.37 Å are not suitable for density diagnostics if the electrons are described by a κ-distribution. We failed to diagnose density from the remaining S X and Ar XIV lines since the observed ratios were higher than the theoretical ranges. This indicates the presence of blends, that are either unknown or cannot be removed due to missing data. Therefore, we used Fe line ratios for this purpose. Typically, the diagnosed densities are lower by ≈ 0.1 dex for the κ-distribution than the densities diagnosed for the Maxwellian distribution. This is due to changes in the ionization and excitation equilibria with κ. The total errors in the determination of density can be up to ≈ 0.3 dex if the temperature of the emitting plasma is unknown.

2.2 Diagnostics from the HOP 226

The suggested diagnostics methods were tested on dataset from own observation proposed for Hinode/EIS, within Hinode Operation Plan (HOP) 226. Data reduction was performed carefully. We selected coronal loop and provided diagnostics of its plasma parameters using specific spectral lines. We found that all plasma parameters diagnosed using different line ratios were almost consistent.

Densities diagnosed using the line ratios of Fe XI and Fe XIII are shown in Fig. 2.1. The temperatures, for which the emissivity of the line reaches its maximum (solid lines) and for temperatures for which the emissivity of the line falls on the 1 % of its maximum (dashed and dot-dashed lines) are used. The mean density for the Maxwellian distribution is diagnosed as $\log(n_e[\mathrm{cm}^{-3}]) = 9.38^{+0.19}_{-0.15}$ and for the κ-distribution with κ=2 as $\log(n_e[\mathrm{cm}^{-3}]) = 9.29^{+0.19}_{-0.15}$.

The diagnostics of κ-distribution is presented in Fig. 2.2. The ratios of Fe XI to Fe XII line intensities have a high sensitivity for diagnostics of κ. Changes in the ionization equilibrium increase the sensitivity to κ, which can then be detected more readily.

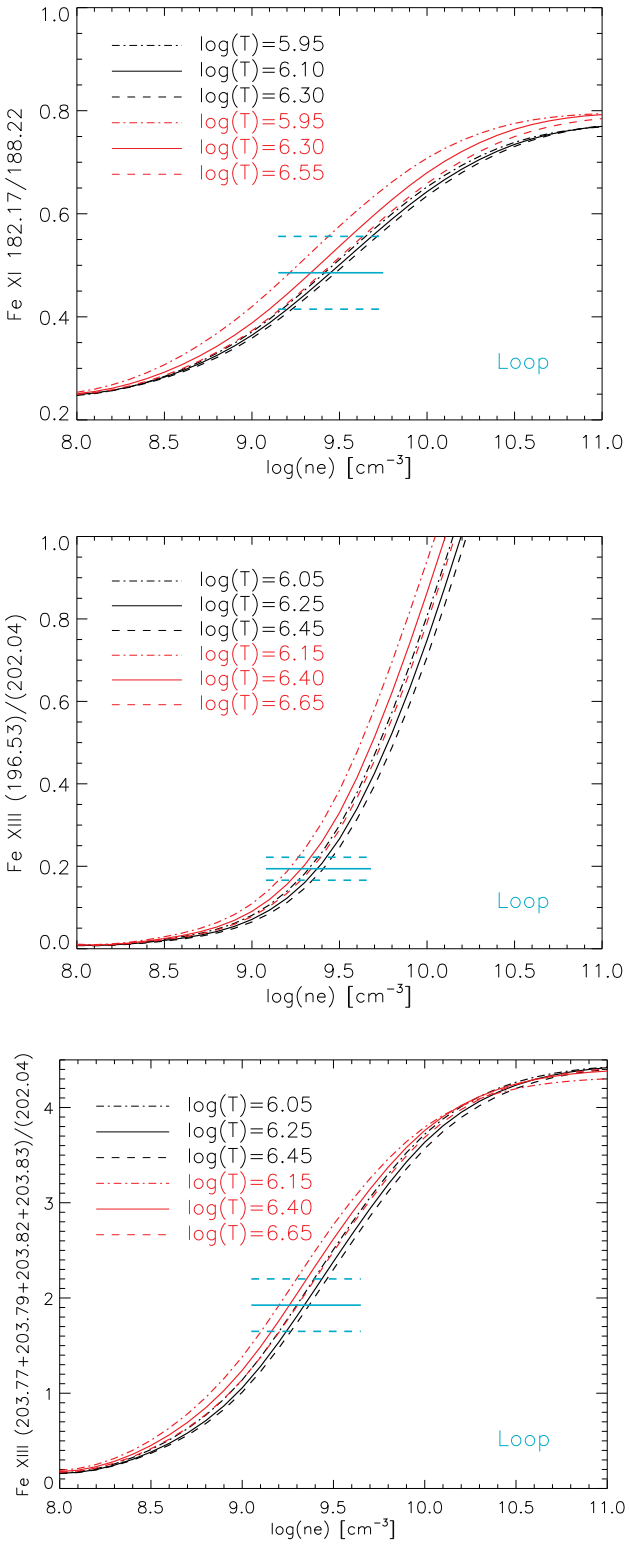

Figure 2.1: Density diagnostics using Fe line ratios. Synthetic intensities for Maxwellian distributions (*black*) and κ=2 distribution (*red*) are displayed. Observed intensity ratios of loop are indicated with their respective errors.

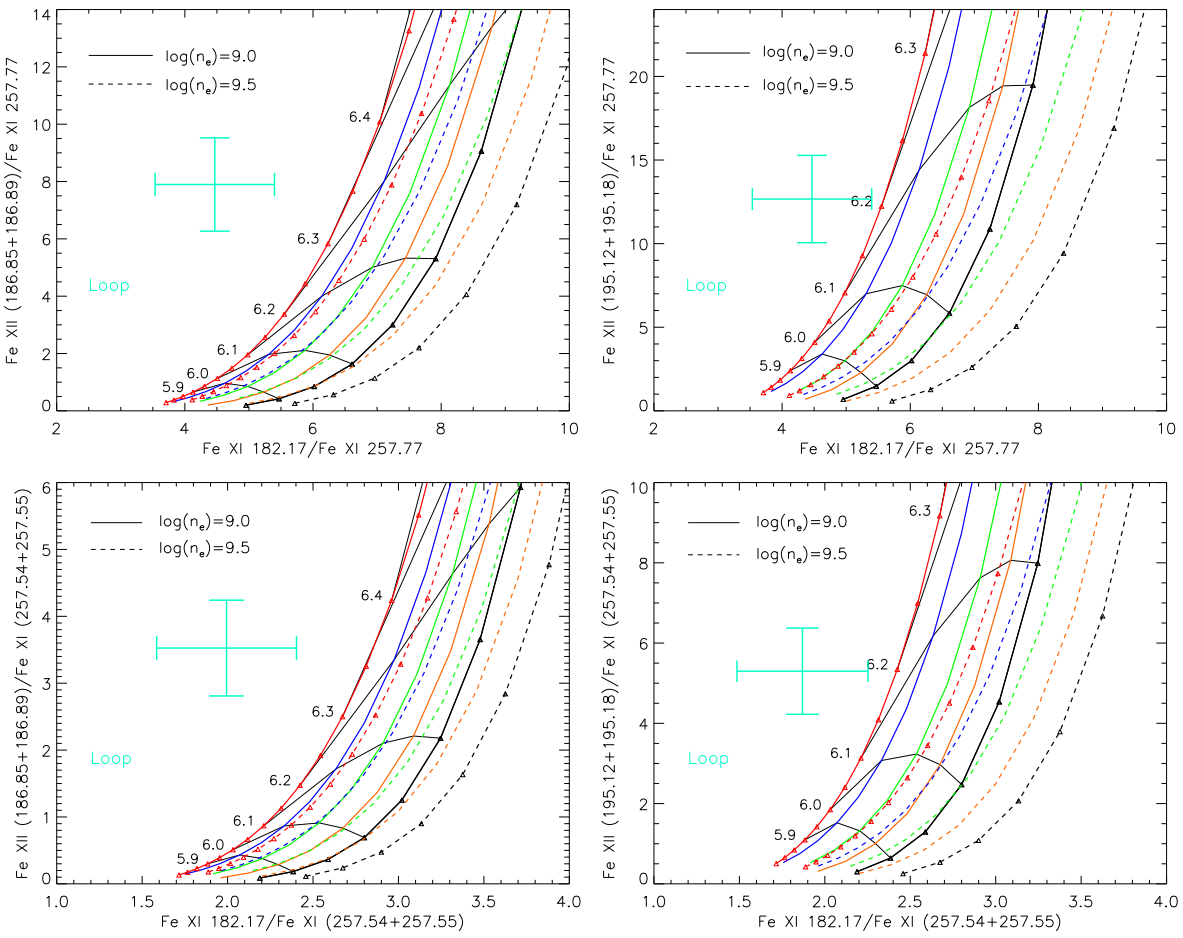

Figure 2.2: Ratio-ratio diagrams for determination of κ from iron lines. Line intensity ratios for the observed loop are indicated by the cross with its error bars. The color coding represents the value of κ: $\kappa = 2$ (red lines), $\kappa = 3$ (blue), $\kappa = 5$ (green), $\kappa = 10$ (yellow), and Maxwellian distribution (black). Points with constant value of $\log(T[\mathrm{K}])$ are connected with thin black lines. Different line styles representing different densities are indicated.

The diagnosed distribution is unlikely to be Maxwellian and value of diagnosed κ-distribution is very close to κ=2 (Fig. 2.2). However, the observed line intensity ratios do not exactly match the predicted ratio-ratio diagrams. The predicted ratio-ratio diagrams were calculated for the diagnosed densities of $\log(n_e[\mathrm{cm}^{-3}]) = 9.0$–$9.5$ and values of $\kappa = 2$, 3, 5, 10, and Maxwellian. This mismatch can be a result of unknown blends or self-blends, lower values of κ in the observed plasmas, or unknown factors. Different ratios of Fe XII to Fe XI line intensities correspond to different temperatures for any distribution (Fig. 2.2) what suggested that plasma could be

multithermal or there could be a problem with atomic data. We note that errors due to photon statistics, calibration errors and uncertainties of atomic data were taken into account in the estimation of error bars in Fig. 2.2. The temperatures diagnosed using individual ratio-ratio diagrams, ≈ 6.1–6.3 are however consistent with typical temperatures detected in coronal loops. Note also that all four ratio-ratio diagrams show consistently that $\kappa < 2$, which may not be a coincidence.

We conclude that the diagnostics presented here do not provide conclusive and unambiguous evidence for the presence of the κ-distributions in the solar corona. However, these results are suggestive, and can represent only one piece of the puzzle that can lead to a more complex picture of the existence of non-Maxwellian distributions in the solar corona (see also Chapter 3). Our study also shown that the observations with higher precision and better spectral resolution, than Hinode/EIS could offer in present time, are needed for a such analysis.

Chapter 3

DEM analysis and the κ-distributions

We investigated the temperature structure of several active region cores and a quiet Sun region under the assumption of the non-Maxwellian κ-distributions. To recover the differential emission measure, we used two methods, namely the Withbroe-Sylwester (W-S) method (Withbroe, 1975; Sylwester et al., 1980) and the regularization method (RIM) (Hannah and Kontar, 2012). We demonstrated that both DEM reconstruction methods give similar solutions. This gives confidence in the validity of the reconstructed DEMs. The reconstructed Maxwellian DEMs for three active region cores and quiet Sun region are in good qualitative agreement with results published by other authors, who use different DEM reconstruction techniques (Warren et al., 2012; Landi and Young, 2010). We shown that the influence of κ-distributions on the DEMs is similar for each of the three active region cores studied. With decreasing κ, the DEMs become more rotund and their peaks are shifted to higher temperatures (Fig. 3.1). This is chiefly a consequence of changes in ionization equilibrium, which also lead to individual lines being formed at wider range of temperatures. The slopes of the EM distributions leftward of its peak do not change appreciably with κ. This suggests that different assumptions on the shape of the electron distribution function do not change the constraints on the coronal heating mechanism. Interpretation of quiet Sun plasma emission may differ for different types of electron distribution assumed. The DEM is found to be multithermal for Maxwellian distribution, but is much less multithermal for $\kappa \approx 2$ (Fig. 3.2).

Our results show that the multithermality of plasma can be a robust result, although the

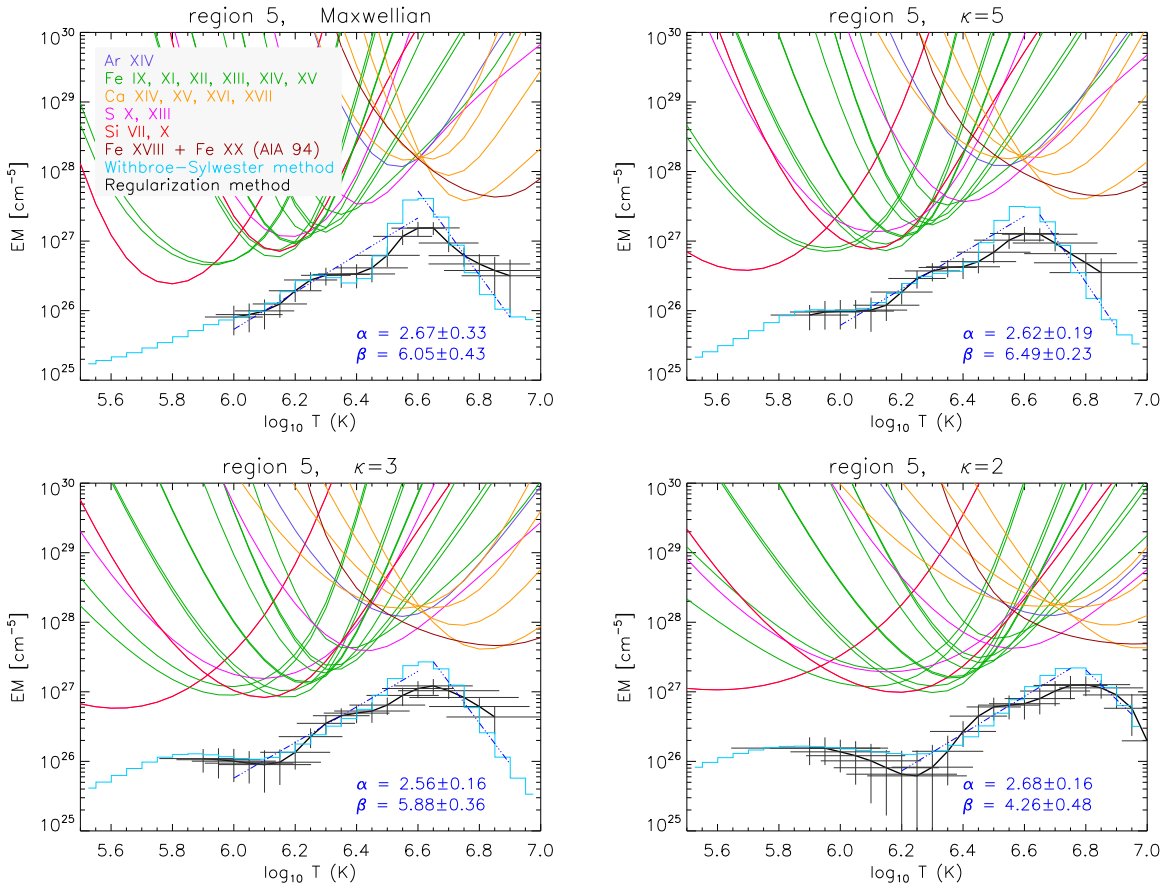

Figure 3.1: EM-loci plots (different colors stand for different ions) and the EM distributions for inter-moss region 5 using the W-S method (light blue line) and the RIM (thick black line). The RIM provide vertical and horizontal error bars. The EM(T) for Maxwellian distribution (*top left*) and κ-distribution with $\kappa = 5$ (*top right*), $\kappa = 3$ (*bottom left*), $\kappa = 2$ (*bottom right*) is shown. The slopes of EMs are indicated by dark blue linear fits. The power-law indexes α and β are listed.

degree of the multithermality is dependent on the region observed and assumed particle distribution. Especially in the active region cores, some constraints on the coronal heating can be derived from DEM reconstruction regardless of the particle microphysics. For example, the relative number of high-energy electrons produced by the coronal heating. This is a somewhat surprising result, since the contribution functions of the individual spectral lines are highly dependent on the assumed distribution function.

This dependency of the line intensities on the shape of the energy distribution calls for a closer scrutiny of the spectroscopic observations. A positive diagnostics of the non-Maxwellian distributions in the solar corona would be a "smoking gun" for the coronal heating process in-

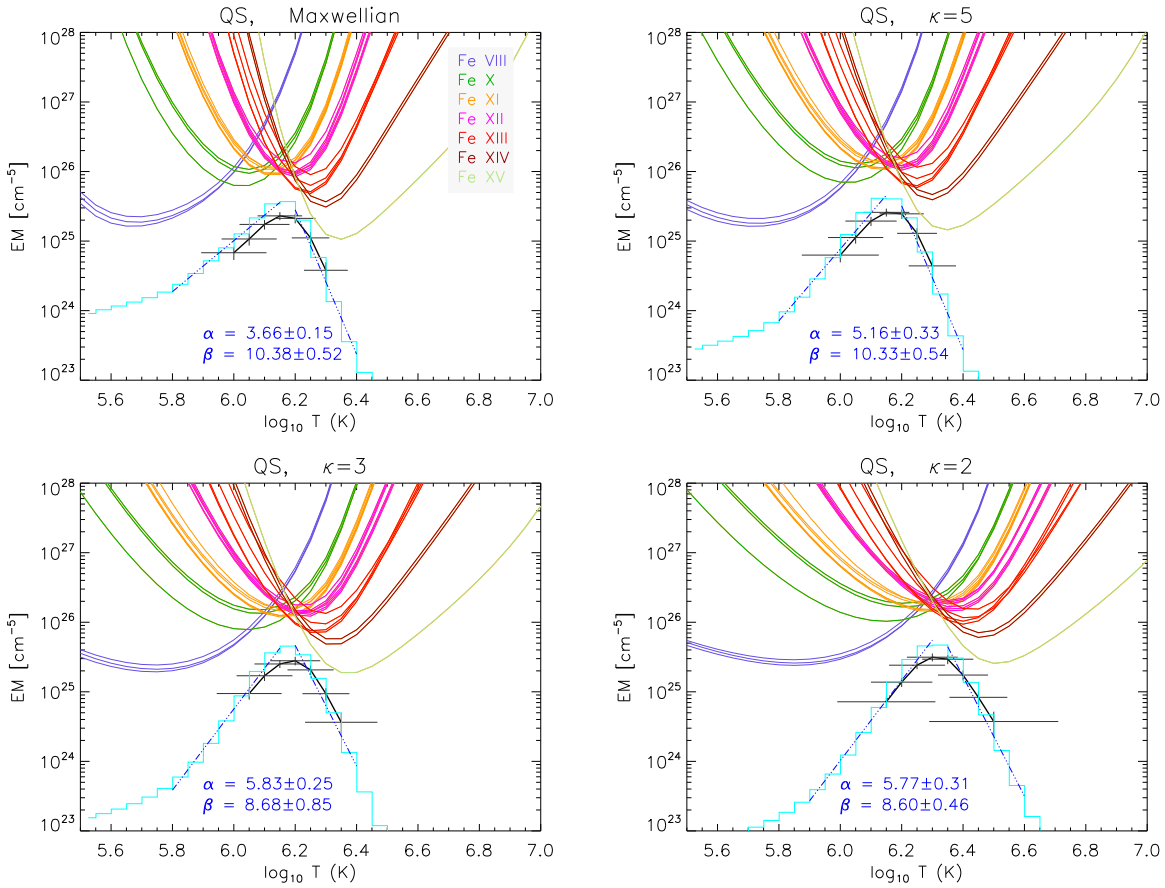

Figure 3.2: The same as Fig. 3.1 but for quiet Sun region.

volved and could possibly help explain the source of the solar wind. Unfortunately, the present spectroscopic observations have limited wavelength coverages and often suffer from instrument and calibration issues preventing the diagnostics, as well as atomic data uncertainties. A comprehensive search for lines suitable for diagnostics of non-Maxwellian distributions in the entire wavelength range is planned. This is important for the interpretation of current and future observations and could also result in improved instrument design.

Bibliography

Brown, C. M., Feldman, U., Seely, J. F., Korendyke, C. M. and Hara, H. (2008), 'Wavelengths and Intensities of Spectral Lines in the 171-211 and 245-291 Å Ranges from Five Solar Regions Recorded by the Extreme-Ultraviolet Imaging Spectrometer (EIS) on Hinode', *Astrophys. J. Suppl. Ser.* **176**, 511–535.

Collier, M. R., Hamilton, D. C., Gloeckler, G., Bochsler, P. and Sheldon, R. B. (1996), 'Neon-20, Oxygen-16, and Helium-4 densities, temperatures, and suprathermal tails in the solar wind determined with WIND/MASS', *Geophys. Res. Lett.* **23**, 1191–1194.

Culhane, J. L., Harra, L. K., James, A. M., Al-Janabi, K., Bradley, L. J., Chaudry, R. A., Rees, K., Tandy, J. A., Thomas, P., Whillock, M. C. R., Winter, B., Doschek, G. A., Korendyke, C. M., Brown, C. M., Myers, S., Mariska, J., Seely, J., Lang, J., Kent, B. J., Shaughnessy, B. M., Young, P. R., Simnett, G. M., Castelli, C. M., Mahmoud, S., Mapson-Menard, H., Probyn, B. J., Thomas, R. J., Davila, J., Dere, K., Windt, D., Shea, J., Hagood, R., Moye, R., Hara, H., Watanabe, T., Matsuzaki, K., Kosugi, T., Hansteen, V. and Wikstol, Ø. (2007), 'The EUV Imaging Spectrometer for Hinode', *Solar Phys.* **243**, 19–61.

Decker, R. B., Krimigis, S. M., Roelof, E. C., Hill, M. E., Armstrong, T. P., Gloeckler, G., Hamilton, D. C. and Lanzerotti, L. J. (2005), 'Voyager 1 in the Foreshock, Termination Shock, and Heliosheath', *Science* **309**, 2020–2024.

Dere, K. P., Landi, E., Mason, H. E., Monsignori Fossi, B. C. and Young, P. R. (1997), 'CHIANTI - an atomic database for emission lines', *Astron. Astrophys. Suppl.* **125**, 149–173.

Dzifčáková, E. (2002), 'The Updated fe Ionization Equilibrium for the Electron K-Distributions', *Solar Phys.* **208**, 91–111.

Dzifčáková, E. (2006), The Modification of Chianti for the Computation of Synthetic Emission Spectra for the Electron Non-Thermal Distributions, *in* 'SOHO-17. 10 Years of SOHO and Beyond', Vol. 617 of *ESA Special Publication*.

Dzifčáková, E. and Dudík, J. (2013), 'H to Zn Ionization Equilibrium for the Non-Maxwellian Electron κ-distributions: Updated Calculations', *Astrophys. J. Suppl. Ser.* **206**, 6.

Dzifčáková, E. and Kulinová, A. (2010), 'The Diagnostics of the κ-Distributions from EUV Spectra', *Solar Phys.* **263**, 25–41.

Dzifčáková, E. and Kulinová, A. (2011), 'Diagnostics of the κ-distribution using Si III lines in the solar transition region', *Astron. Astrophys.* **531**, A122.

Dzifčáková, E. and Mason, H. (2008), 'Computation of Non-Maxwellian Electron Excitation Rates for Ions of Astrophysical Interest: Fe xv A Test Case', *Solar Phys.* **247**, 301–320.

Feldman, U., Landi, E. and Doschek, G. A. (2007), 'Diagnostics of Suprathermal Electrons in Active-Region Plasmas Using He-like UV Lines', *Astrophys. J.* **660**, 1674–1682.

Hannah, I. G. and Kontar, E. P. (2012), 'Differential emission measures from the regularized inversion of Hinode and SDO data', *Astron. Astrophys.* **539**, A146.

Kašparová, J. and Karlický, M. (2009), 'Kappa distribution and hard X-ray emission of solar flares', *Astron. Astrophys.* **497**, L13–L16.

Kosugi, T., Matsuzaki, K., Sakao, T., Shimizu, T., Sone, Y., Tachikawa, S., Hashimoto, T., Minesugi, K., Ohnishi, A., Yamada, T., Tsuneta, S., Hara, H., Ichimoto, K., Suematsu, Y., Shimojo, M., Watanabe, T., Shimada, S., Davis, J. M., Hill, L. D., Owens, J. K., Title, A. M., Culhane, J. L., Harra, L. K., Doschek, G. A. and Golub, L. (2007), 'The Hinode (Solar-B) Mission: An Overview', *Solar Phys.* **243**, 3–17.

Landi, E. and Young, P. R. (2010), 'The Relative Intensity Calibration of Hinode/EIS and SOHO/SUMER', *Astrophys. J.* **714**, 636–643.

Landi, E., Young, P. R., Dere, K. P., Del Zanna, G. and Mason, H. E. (2013), 'CHIANTI - An Atomic Database for Emission Lines. XIII. Soft X-Ray Improvements and Other Changes', *Astrophys. J.* **763**, 86.

Le Chat, G., Issautier, K., Meyer-Vernet, N. and Hoang, S. (2011), 'Large-Scale Variation of Solar Wind Electron Properties from Quasi-Thermal Noise Spectroscopy - Ulysses Measurements', *Solar Phys.* **271**, 141–148.

Leubner, M. P. (2002), 'A Nonextensive Entropy Approach to Kappa-Distributions', *Astrophys. Space Sci.* **282**, 573–579.

Livadiotis, G. and McComas, D. J. (2009), 'Beyond kappa distributions: Exploiting Tsallis statistical mechanics in space plasmas', *Journal of Geophysical Research (Space Physics)* **114**, 11105.

Livadiotis, G. and McComas, D. J. (2012), 'Non-equilibrium Thermodynamic Processes: Space Plasmas and the Inner Heliosheath', *Astrophys. J.* **749**, 11.

Livadiotis, G. and McComas, D. J. (2013), 'Understanding Kappa Distributions: A Toolbox for Space Science and Astrophysics', *Space Sci. Rev.* **175**, 183–214.

Maksimovic, M., Pierrard, V. and Riley, P. (1997), 'Ulysses electron distributions fitted with Kappa functions', *Geophys. Res. Lett.* **24**, 1151–1154.

Oka, M., Ishikawa, S., Saint-Hilaire, P., Krucker, S. and Lin, R. P. (2013), 'Kappa Distribution Model for Hard X-Ray Coronal Sources of Solar Flares', *Astrophys. J.* **764**, 6.

Owocki, S. P. and Scudder, J. D. (1983), 'The effect of a non-Maxwellian electron distribution on oxygen and iron ionization balances in the solar corona', *Astrophys. J.* **270**, 758–768.

Phillips, K. J. H., Feldman, U. and Landi, E. (2008), Cambridge University Press.
URL: *http://dx.doi.org/10.1017/CBO9780511585968.017*

Pinfield, D. J., Keenan, F. P., Mathioudakis, M., Phillips, K. J. H., Curdt, W. and Wilhelm, K. (1999), 'Evidence for Non-Maxwellian Electron Energy Distributions in the Solar Transition Region: Si III Line Ratios from SUMER', *Astrophys. J.* **527**, 1000–1008.

Scudder, J. D. and Karimabadi, H. (2013), 'Ubiquitous Non-thermals in Astrophysical Plasmas: Restating the Difficulty of Maintaining Maxwellians', *Astrophys. J.* **770**, 26.

Shoub, E. C. (1983), 'Invalidity of local thermodynamic equilibrium for electrons in the solar transition region. I - Fokker-Planck results', *Astrophys. J.* **266**, 339–369.

Sylwester, J., Schrijver, J. and Mewe, R. (1980), 'Multitemperature analysis of solar X-ray line emission', *Solar Phys.* **67**, 285–309.

Tsallis, C. (2009), *Introduction to Nonextensive Statistical Mechanics*, Springer New York.

Vasyliunas, V. M. (1968), 'A Survey of Low-Energy Electrons in the Evening Sector of the Magnetosphere with OGO 1 and OGO 3', *J. Geophys. Res.* **73**, 2839.

Warren, H. P., Winebarger, A. R. and Brooks, D. H. (2012), 'A Systematic Survey of High-temperature Emission in Solar Active Regions', *Astrophys. J.* **759**, 141.

Withbroe, G. L. (1975), 'The analysis of XUV emission lines', *Solar Phys.* **45**, 301–317.

Young, P. R. (2007), 'Density diagnostics for eis'.
URL: *http://www.pyoung.org/hinode/recommended-diags.pdf*

Zouganelis, I. (2008), 'Measuring suprathermal electron parameters in space plasmas: Implementation of the quasi-thermal noise spectroscopy with kappa distributions using in situ Ulysses/URAP radio measurements in the solar wind', *Journal of Geophysical Research (Space Physics)* **113**, 8111.